Laser and Particle Beams

cambridge.org/lpb

Improvement of ion acceleration in radiation pressure acceleration regime by using an external strong magnetic field

H. Cheng[1], L. H. Cao[1,2,3], J. X. Gong[2], R. Xie[2], C. Y. Zheng[1,2,3] and Z. J. Liu[1,2]

[1]Institute of Applied Physics and Computational Mathematics, Beijing, 100088, China; [2]Center of Applied Physics and Technology, HEDPS, and SKLNPT, School of Physics, Peking University, Beijing 1000871, China and [3]IFSA Collaborative Innovation Center, Shanghai Jiao Tong University, Shanghai, 200240, China

Research Article

Cite this article: Cheng H, Cao LH, Gong JX, Xie R, Zheng CY, Liu ZJ (2019). Improvement of ion acceleration in radiation pressure acceleration regime by using an external strong magnetic field. *Laser and Particle Beams* **37**, 217–222. https://doi.org/10.1017/S026303461900034X

Received: 14 January 2019
Revised: 22 January 2019
Accepted: 19 March 2019

Key words:
External magnetic fields; PIC simulations; proton acceleration; proton divergence promotions; radiation pressure acceleration

Author for correspondence:
Lihua Cao, Institute of Applied Physics and Computational Mathematics, Beijing 100088, China. E-mail: cao_lihua@iapcm.ac.cn

Abstract

Two-dimensional particle-in-cell (PIC) simulations have been used to investigate the interaction between a laser pulse and a foil exposed to an external strong longitudinal magnetic field. Compared with that in the absence of the external magnetic field, the divergence of proton with the magnetic field in radiation pressure acceleration (RPA) regimes has improved remarkably due to the restriction of the electron transverse expansion. During the RPA process, the foil develops into a typical bubble-like shape resulting from the combined action of transversal ponderomotive force and instabilities. However, the foil prefers to be in a cone-like shape by using the magnetic field. The dependence of proton divergence on the strength of magnetic field has been studied, and an optimal magnetic field of nearly 60 kT is achieved in these simulations.

Introduction

Ion acceleration *via* laser–plasma interaction has attracted much attention due to its lower cost and convenience compared with the conventional ion accelerator. The utilization of an ultra-intense laser provides an extremely strong electromagnetic field and an ultra-high acceleration rate for ion acceleration. This has generated an alternative of the conventional particle acceleration and has been used widely in numerous applications of high-energy ions, such as ion sources (Daido *et al.*, 2012; Wagner *et al.*, 2016), radiography (Edwards *et al.*, 2002), hadron therapy of diseases (Bulanov and Khoroshkov 2002), and fast ignition inertial confinement fusion (Roth *et al.*, 2001). It has also given a strong motivation to research pertinent questions (Wang *et al.*, 2013; Kim *et al.*, 2016; Honrubia *et al.*, 2017; Yogo *et al.*, 2017).

The basic scheme of ion acceleration *via* laser–plasma interaction is the relativistic flying mirror concept in which the ponderomotive force of laser pushes electrons away from rear surface of target when an ultra- intense laser pulse ejects into a plasma or a foil. The slap of electrons accelerated by strong electromagnetic waves to nearly light speed forms a strong charge separation field to pull ions to co-propagate with the laser pulse. Based on this frame, the mechanisms of ion acceleration *via* laser–plasma interaction include mainly the following aspects: Target normal sheath acceleration (Hatchett *et al.*, 2000; Wilks *et al.*, 2001; Mora, 2003), radiation pressure acceleration (RPA) (Esirkepov *et al.*, 2004; Klimo *et al.*, 2008; Robinson *et al.*, 2008; Yan *et al.*, 2009), Coulomb explosion (Kovalev and Bychenkov 2003; Bulanov *et al.*, 2008), and so on. In this paper, we will focus on the enhancement of ion acceleration *via* RPA by using an external longitudinal magnetic field. RPA is one of the most efficient mechanisms because nearly all the laser energy is transferred to ions. When the electric field inspired by a laser is nearly the same as the charge separation field, which is defined as $E_m = 2\pi e n_e l$ where e, n_e, and l are charge of electron, electron density, and the thickness of foil, ions and electrons will move together with the laser pulse. According to the double Doppler effect, the laser reflected by the plasma mirror will get a downshift of frequency $\Delta\omega = (1 - 1/4\gamma^2)\omega_L$. This means that each photon energy transferred to ions is referred to $\Delta\varepsilon = \hbar\Delta\omega$, where γ and ω_L are the Lorentz factor of plasma mirror and frequency of laser, respectively. In the relativistic regime, the velocity of electron-ion layer is almost equal to light speed, making $\gamma \gg 1$. This will lead to an almost complete laser energy transferred to ions, making RPA a promising approach to obtain high-energy ions. However, some limitations of ion-beam quality such as (i) transverse target expansion (Dollar *et al.*, 2012), (ii) slightly focused laser group velocity (Bulanov *et al.*, 2015), and (iii) target transparency (Macchi *et al.*, 2009) greatly harm the quality of proton *via* RPA. In this paper, we will focus on the influence of the transverse target expansion which results in reduction of electron density. This tends to terminate the process of RPA ahead of time. It may excite some harmful transverse instabilities such as Rayleigh–Taylor like instability (Pegoraro and Bulanov, 2007; Palmer *et al.*, 2012) and Weibel-like instability (Yoon and Davidson 1987). Furthermore, deconstruction of foil

CAMBRIDGE UNIVERSITY PRESS

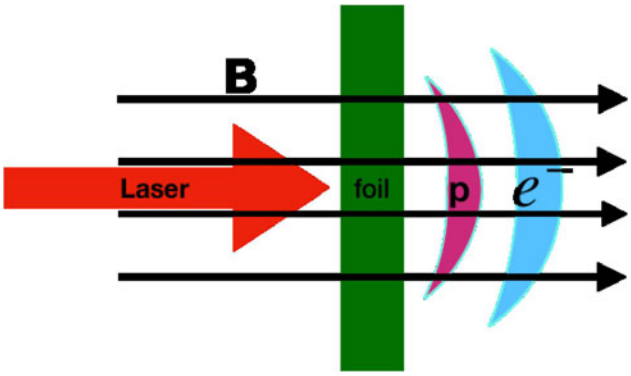

Fig. 1. A laser pulse with the normalized laser amplitude of $a_0 = 70$ ejects into a hydrogen foil with an external longitudinal magnetic field. The wavelength of laser is 1 μm and the density of hydrogen foil is $80n_c$, where n_c is the critical density ($1.1 \times 10^{21}/\text{cm}^3$).

caused by the transverse expansion enlarges the proton divergence and reduces the quality of proton. Significant work has been devoted to decreasing the proton divergence and improving the quality of proton (Weng *et al.*, 2015; Zou *et al.*, 2015; Shen *et al.*, 2017).

A magnetic field of over several kilotesla has been obtained with a capacitor-coil target driven by a high-power laser. The strength of magnetic field has increased from 60 T to 1.5 kT over the past 30 years (Daido *et al.*, 1986; Fujioka *et al.*, 2013; Abe *et al.*, 2018; Nakamura *et al.*, 2018). Therefore, it is expectable to obtain a higher magnetic field with the rapid development of laser technology and innovative laser–plasma research in the future. The investigation in combination of plasma and strong magnetic field has also attracted much attention (Arefiev *et al.*, 2016; Stark *et al.*, 2016; Gong *et al.*, 2017).

In this paper, 2D particle-in-cell (PIC) simulations have been carried out to investigate ion acceleration in RPA regime with an external magnetic field. The divergence of proton has been improved greatly in the RPA regime by using an external longitudinal magnetic field. In the absence of magnetic field, the foil develops into a bubble-like shape from the simulations. The foil prefers to be in a cone-like shape by using the magnetic field. Furthermore, the dependence of proton divergence on the strength of magnetic field has been studied, and an optimal magnetic field of nearly 60 kT is achieved under the conditions considered in this paper.

Simulation and results

In order to investigate ion acceleration *via* RPA with a longitudinal strong magnetic field, some two-dimensional PIC simulations have been performed using the EPOCH code (Arber *et al.*, 2015). The simulation scheme is shown in Figure 1.

A circularly polarized laser pulse irradiates the hydrogen foil, which is transversely Gaussian as $E_L(y) = E_0\exp(-y^2/r^2)$, with a full width at half maximum (FWHM) of $r = 10\lambda$ and a laser

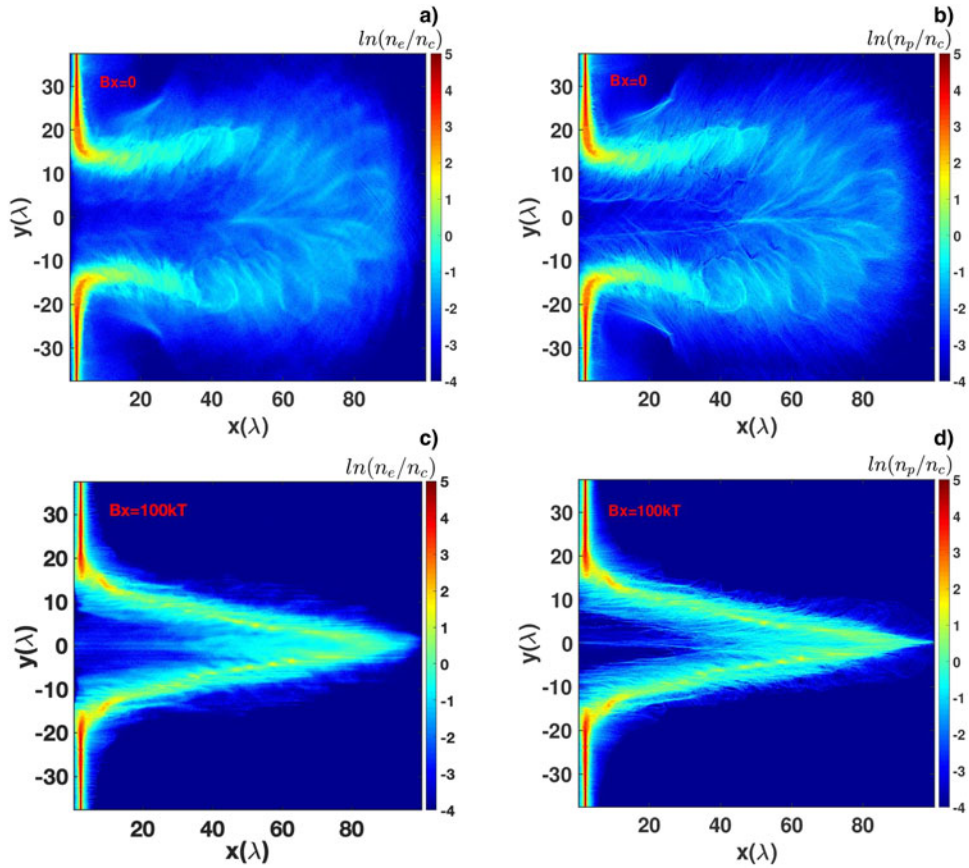

Fig. 2. The density of electrons (a and c) and protons (b and d) without magnetic field (a and b) and with magnetic field (c and d), $B_x = 100$ kT. The density of electrons and protons are normalized to the critical density $n_c = 1.1 \times 10^{21}/\text{cm}^3$ at $140T_L$ in the simulations.

https://doi.org/10.1017/S026303461900034X Published online by Cambridge University Press

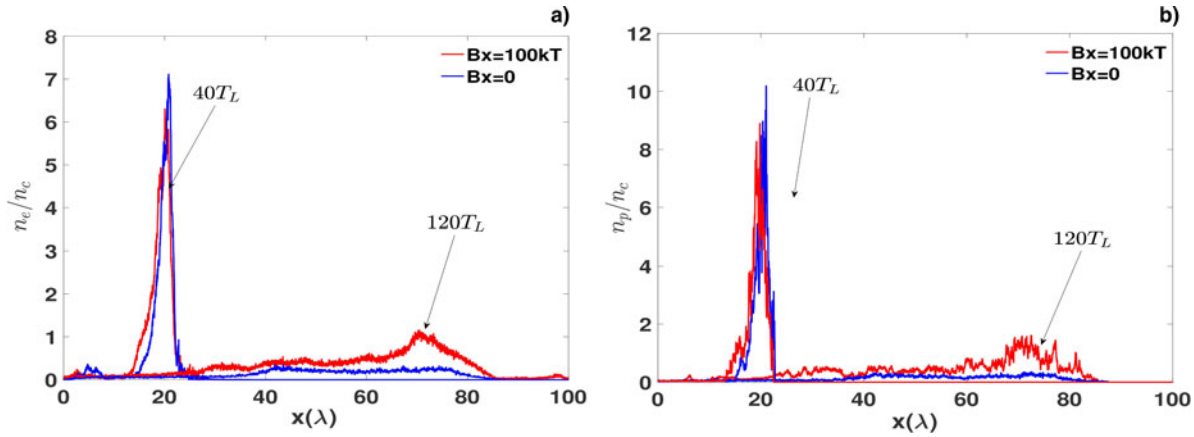

Fig. 3. Spatial evolution of density of electrons (a) and protons (b) along x-axis when $y = 0$ in the presence of magnetic field (red line) and in the absence of magnetic field (blue line) at $40T_L$ and $140T_L$. The spatial variable is normalized by the wavelength of laser and the density of charged particles is normalized by the critical density.

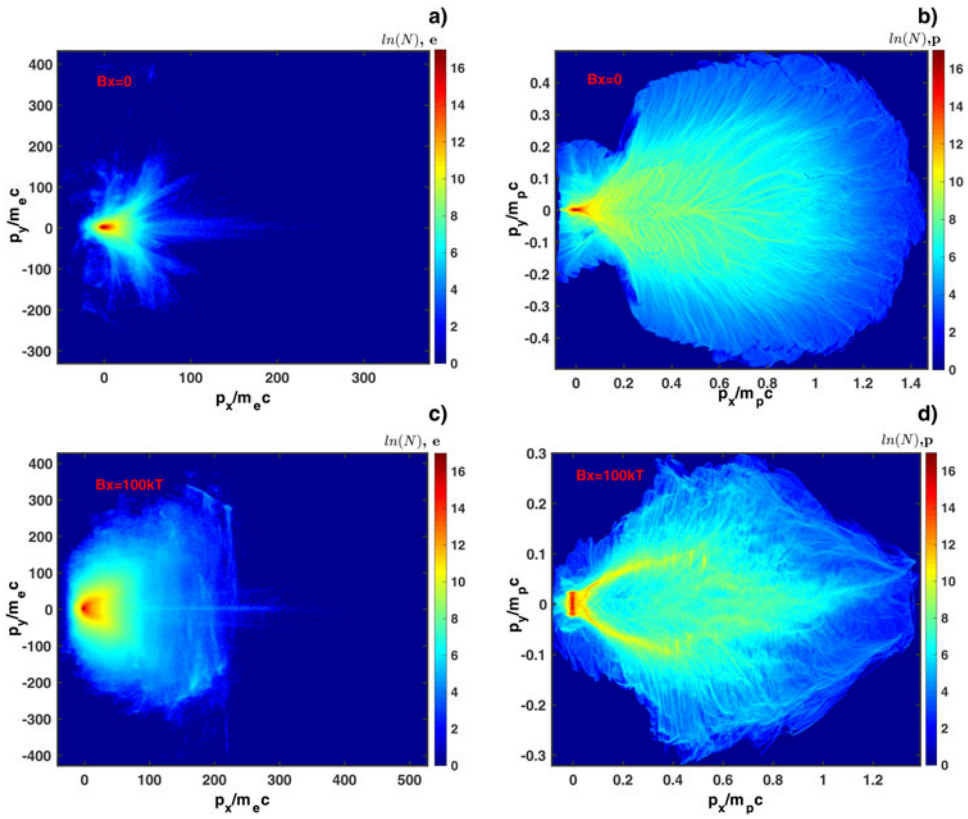

Fig. 4. The distribution in the momentum of electrons (a and c) and protons (b and d). (a) and (b) are the cases without magnetic field and (c) and (d) are the one with magnetic field (B_x = 100 kT). The momentum of particles is normalized by the product of static mass and laser speed ($m_{p(e)}c$), where m_p and m_e is the mass of electron and proton, respectively.

duration of 15 T_L, where E_0 has been regarded as the electric field amplitude of the laser pulse, and λ is the wavelength of 1 μm, and T_L is the normalized laser amplitude of $a_0 = (eE_0)/(m_e c\omega_0) = 70$, where m_e, c, and ω_0 are the mass of electron, the speed of light in vacuum, and the local frequency of light, respectively.

In our two-dimensional PIC simulations, the dimensions of the simulation box are 80 μm × 140 μm with 3200 × 5600 cells. There are 50 particles for each cell. The laser pulse ejects into the simulation box from the left boundary. The hydrogen foil locates at 2 μm < x < 2.5 μm, with a foil thickness of $D = 0.5$ μm, and the density of electron and proton is homogeneously $80n_c$, where $n_c = 1.1 \times 10^{21}$ /cm^3 is the critical density for the laser pulse. To study the effect of a strong magnetic field on ion acceleration *via* RPA, we compare two cases with or without magnetic field applied in the longitudinal direction. The comparison of electron and ion density is shown in Figure 2.

https://doi.org/10.1017/S026303461900034X Published online by Cambridge University Press

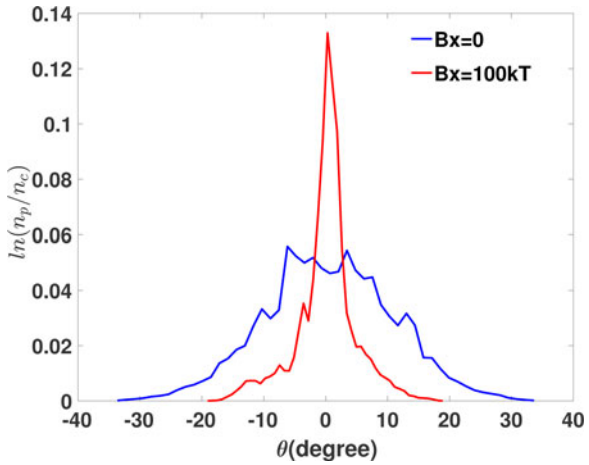

Fig. 5. The distribution of angle and density of protons whose energy is larger than 300 MeV with magnetic field (red line, $B_x = 100$ kT) and without magnetic field (blue line). Here θ is the angle between the momentum of protons and the *x*-axis.

As shown in Figure 2a and 2b, the foil is in bubble-like shape in the absence of a magnetic field. However, electrons expand comparatively more slowly with a longitudinal magnetic field of $B_x = 100$ kT as shown in Figure 2c. In this case, the foil reveals a cone-like structure as shown in Figure 2c and 2d. The density of charged particles plays a key role in RPA. Reduction of electron areal density greatly harms the quality of proton. As shown in Figure 3a, the density of electrons decreases from $80n_c$ to nearly $7n_c$ along *x*-axis when $y = 0$ area in both cases. In the absence of a magnetic field, the electron density is nearly $0.2n_c$ at $140T_L$. And the electron density with a magnetic field is near $1.1n_c$. It indicates a strong longitudinal field which greatly helps to restrict the transverse expansion and the structure of foil has also been changed into a cone-like shape. As shown in Figure 3b, the proton density with a magnetic field is almost seven times more than that without a magnetic field.

Figure 4 presents the comparison of proton momentum distribution to study the effect of magnetic field on the divergence of proton. θ is the emission angle. As shown in Figure 4a and 4c, the configuration of electrons demonstrates that transverse expansion of electrons has been indeed suppressed by introducing of a longitudinal magnetic field. We define $p_x(e)$ and $p_y(e)$ as the longitudinal momentum and the transverse momentum of electrons, and $p_x(p)$ and $p_y(p)$ as the longitudinal momentum and the transverse momentum of proton. Although the maximum $p_y(e)$ in Figure 4a and 4c are almost the same, the maximum $p_x(e)$ in Figure 4c with a magnetic field has been promoted. And maxima $p_x(p)$ in Figure 4b and 4d are almost the same in both cases, but the maximum $p_y(p)$ in Figure 4d with magnetic field is $0.1m_pc$ less than that in Figure 4b. This may contribute to the inhibition of the electron transverse motion. When electrons are driven by the longitudinal magnetic field, the transverse motion of electrons will be suppressed. And this restrains electrons to pull protons in the transverse direction and finally reduces the transverse momentum of protons. Meanwhile,

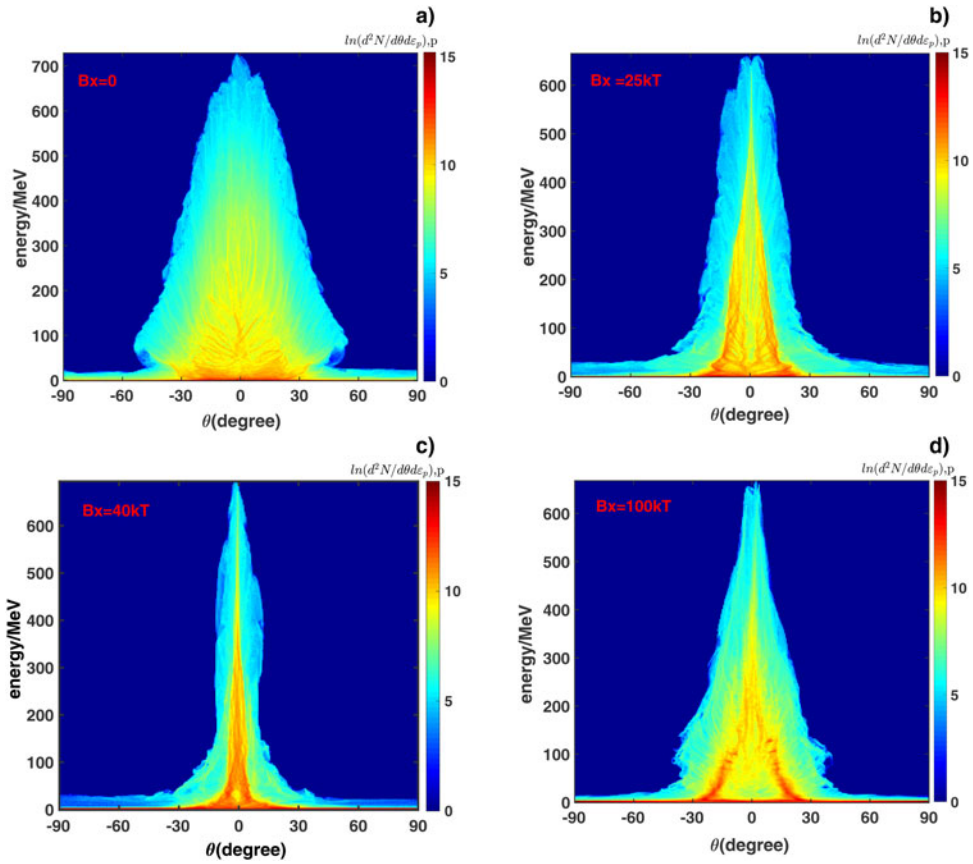

Fig. 6. The proton distribution as a function of energy and emission angle with different magnetic fields at $140T_L$. The magnetic field used is (a) 0 kT, (b) 25 kT, (c) 40 kT, and 100 kT. θ is the angle between the momentum of protons and the *x*-axis.

https://doi.org/10.1017/S026303461900034X Published online by Cambridge University Press

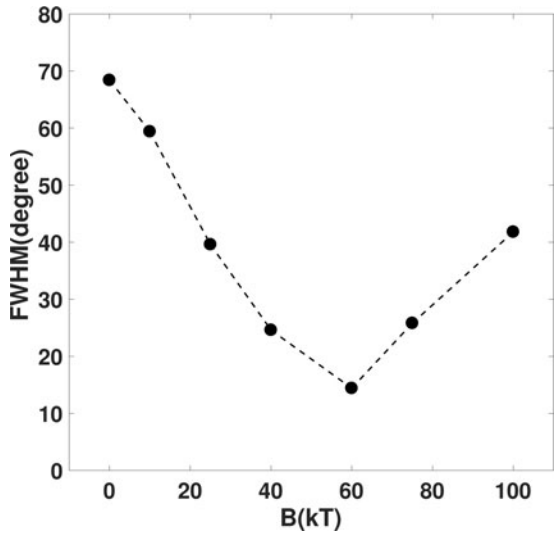

Fig. 7. The distribution of the range of proton emission angle whose energy is 300 MeV as a function of magnetic field. The magnitude if magnetic field varies from 0 to 100 kT.

the magnetic field has little impact on the longitudinal acceleration. However, $p_y(p)$ in Figure 4d is roughly $0.3m_pc$ and $0.4m_pc$ in Figure 4b. The maximum proton energy is 660 MeV with a magnetic field, and it is 700 MeV in the absence of a magnetic field. The notable improvement to divergence of proton beam and enhancement of the areal density are achieved, even if the maximum energy decreases slightly in the presence of magnetic field. As shown in Figure 4b and 4d, the proton distributions in the momentum are quite different in both cases. Therefore, the divergence of ion beams improved remarkably with an external magnetic field.

Now we focus on the proton divergence. The angular distribution of protons with energy larger than 300 MeV is shown in Figure 5. The FWHM of the proton angular distribution with a magnetic field is about 4° and it is 20° without a magnetic field. The distribution peaks at 0°. Restriction of electrons offered by the magnetic field impacts on directly the motion of protons and improves remarkably the proton divergence. Then we will study the dependence of proton divergence on strength of magnetic field. In the following simulations, the magnitudes of magnetic field are assumed to be 25, 40, and 100 kT. The proton distribution as a function of energy and emission angle at $140T_L$ is given in Figure 6. As shown in Figure 6b–6d, the maximum energy of protons is almost 660 MeV and is slightly less than that in Figure 6a. It can be seen that the maximum proton energy is almost the same in different strengths of magnetic field.

As shown in Figure 6, the emission angle of proton depends on the strength of magnetic field. The full width of the distribution envelop of Figure 6 at 300 MeV has been used to investigate the dependence of proton divergence on the strength of magnetic field. As shown in Figure 7, the range of proton emission angle whose energy is 300 MeV reduces to the minimum of 15° at 60 kT from 70° without magnetic field, then increases to 42° at 100 kT. From Figure 7, there exists an optimal magnetic field of 60 kT to achieve the minimum proton divergence. The intense magnetic field is required to overcome the transverse expansion. In fact, the foil is developing into a cone-like shape once the magnetic field exceeds the optimal magnetic field as shown in Figure 2c and 2d. In this case, the majority of protons move along the cone-like shape, which leads to increasing emission angle of proton.

Conclusion

We have implied several two-dimensional PIC simulations to investigate the effect of an external longitudinal magnetic field on RPA. Under the conditions of these simulations, with a strong magnetic field, the foil of $n_0 = 80n_c$ pushed by a laser of $a_0 = 70$ will become a cone-like shape instead of a bubble-like shape in the absence of a magnetic field. The density of the charged particle is almost seven times more than that without a magnetic field. It reveals that the transverse expansion of electrons has been suppressed by a strong longitudinal magnetic field. This greatly helps to improve the proton divergence. The dependence of proton divergence on the strength of a magnetic field has been studied, and an optimal magnetic field of nearly 60 kT is achieved in these simulations. It is expectable to obtain such a magnetic field in the future with the rapid development of new technology, although the required magnetic field of dozens of kilotesla is currently unachievable. Therefore, applying an external magnetic field *via* RPA is potentially promising to improve the quality of protons.

Author ORCIDs. H. Cheng, https://orcid.org/0000-0003-1511-6017.

Acknowledgment. The authors would like to thank the useful discussion of J. Q. Yu and X. Q. Yan. This work was supported by the National Natural Science Foundation of China (Grand Nos. 11875091 and 11475030) and the National Key Research and Development Program of China (Grant No. 2016YFA0401100).

References

Abe Y, Law KFF, Korneev P, Fujioka S, Kojima S, Lee SH, Sakata S, Matsuo K, Oshima A, Arikawa Y, Yogo A, Nakai A, Norimatsu T, Humiers E, Santos JJ, Kondo K, Sunahara A, Gus'kov S and Tikhonchuk V (2018) Whispering gallery effect in relativistic optics. *JETTP Letters* **107**, 351–354.

Arber TD, Bennett K, Brady CS, Lawrence-Douglas A, Ramsay MG, Sircombe NJ, Gillies P, Evans RG, Schmitz H, Bell AR and RIdgers CP (2015) Contemporary particle-in-cell approach to laser-plasma modelling. *Plasma Physics and Controlled Fusion* **5**, 113001.

Arefiev A, Toncian T and Fiksel G (2016) Enhanced proton acceleration in an applied longitudinal magnetic field. *New Journal of Physics* **18**, 105011.

Bulanov SV and Khoroshkov VS (2002) Feasibility of using laser ion accelerators in proton therapy. *Plasma Physics Reports* **28**, 453.

Bulanov SS, Brantov A, Bychenkov VY, Chvykov V, Kalinchenko G, Matsuoka T, Rousseau P, Reed S, Yanovsky V, Litzenberg DW, Krushelnick K and Maksimchuk A (2008) Accelerating monoenergetic protons from ultrathin foils by flat-top laser pulses in the directed-Coulomb-explosion regime. *Physical Review E* **78**, 026412.

Bulanov SS, Esarey E, Schroeder CB, Bulanov SV, Esirkepov TZ, Kando M, Pegoraro F and Leemans WP (2015) Enhancement of maximum attainable ion energy in the radiation pressure acceleration regime using a guiding structure. *Physical Review Letters* **114**, 105003.

Daido H, Miki F, Mima K, Fujita M, Sawai K, Fujita H, Kitagawa Y, Nakai S and Yamanaka C (1986) Generation of a strong magnetic field by an intense CO_2 laser pulse. *Physical Review Letters* **56**, 846–849.

Daido H, Nishiuchi M and Pirozhkov AS (2012) Review of laser-driven ion sources and their applications. *Reports of Progress in Physics* **75**, 056401.

Dollar F, Zulick C, Thomas AGR, Chvykov V, Davis J, Kalinchenko G, Matsuoka T, McGuffey C, Petrov GM, Willingale L, Yanovsky V, Maksimchuk A and Krushelnick K (2012) Finite spot effects on radiation pressure acceleration from intense high-contrast laser interactions with thin targets. *Physical Review Letters* **108**, 175005.

https://doi.org/10.1017/S026303461900034X Published online by Cambridge University Press

Edwards RD, Sinclair MA, Goldsack TJ, Krushelnick K, Beg FN, Clark EL, Dangor AE, Najmudin Z, Tatarakis M, Walton B, Zepf M, Ledingham KWD, Spencer I, Norreys PA, Clarke RJ, Kodama R, Toyama Y and Tampo M (2002) Characterization of a gamma-ray source based on a laser-plasma accelerator with applications to radiography. *Applied Physics Letters* **80**, 2129–2131.

Esirkepov T, Borghesi M, Bulanov SV, Mourou G and Tajima T (2004) Highly efficient relativistic-ion generation in the laser-piston regime. *Physical Review Letters* **92**, 175003.

Fujioka S, Zhang Z, Ishihara K, Shigemori K, Hironaka Y, Johzaki T, Sunahara A, Yamamoto N, Nakashima H, Watanabe T, Shiraga H, Nishimura H and Azechi H (2013) Kilotesla magnetic field due to a capacitor-coil target driven by high power laser. *Scientific Reports* **3**, 1170.

Gong JX, Cao LH, Pan KQ, Xiao KD, Wu D, Zheng CY, Liu ZJ and He XT (2017) Enhancing the electron acceleration by a circularly polarized laser interaction with a cone-target with an external longitudinal magnetic field. *Physics of Plasmas* **24**, 033103.

Hatchett SP, Brown CG, Cowan TE, Henry EA, Johnson JS, Key MH, Koch JA, Langdon AB, Lasinski BF, Lee RW, Mackinnon AJ, Pennington DM, Perry MD, Phillips TW, Roth M, Sangster TC, Singh MS, Snavely RA, Stoyer MA, Wilks SC and Yasuike K (2000) Electron, photon, and ion beams from the relativistic interaction of petawatt laser pulses with solid targets. *Physics of Plasmas* **7**, 2076.

Honrubia JJ, Morace A and Murakami M (2017) On the intense proton beam generation and transport in hollow cones. *Matter and Radiation at Extremes* **2**, 28.

Kim IJ, Pae KH, Choi IW, Lee CL, Kim HT, Singhal H, Sung JH, Lee SK, Lee HW, Nickles PV, Jeong TM, Kim CM and Nam CH (2016) Radiation pressure acceleration of protons to 93 MeV with circularly polarized petawatt laser pulses. *Physics of Plasmas* **23**, 070701.

Klimo O, Psikal J, Limpouch J and Tikhonchuk VT (2008) Monoenergetic ion beams from ultrathin foils irradiated by ultrahigh-contrast circularly polarized laser pulses. *Physical Review Accelerators and Beams* **11**, 031301.

Kovalev VF and Bychenkov VY (2003) Analytic solutions to the Vlasov equations for expanding plasmas. *Physical Review Letters* **90**, 185004.

Macchi A, Veghini S and Pegoraro F (2009) "Light Sail" acceleration reexamined. *Physical Review Letters* **103**, 085003.

Mora P (2003) Plasma expansion into a vacuum. *Physical Review Letters* **90**, 185002.

Nakamura D, Ikeda A, Sawabe H, Matsuda YH and Takeyama S (2018) Record indoor magnetic field of 1200 T generated by electromagnetic flux-compression. *Review of Scientific Instruments* **189**, 095106.

Palmer CAJ, Schreiber J, Nagel SR, Dover NP, Bellei C, Beg FN, Bott S, Clarke RJ, Dangor AE, Hassan SM, Hilz P, Jung D, Kneip S, Mangles SPD, Lancaster KL, Rehman A, Robinson APL, Spindloe C, Szerypo J, Tatarakis M, Yeung M, Zepf M and Najmudin Z (2012) Rayleigh–Taylor instability of an ultrathin foil accelerated by the radiation pressure of an intense laser. *Physical Review Letters* **108**, 225002.

Pegoraro F and Bulanov SV (2007) Photon bubbles and ion acceleration in a plasma dominated by the radiation pressure of an electromagnetic pulse. *Physical Review Letters* **99**, 065002.

Robinson APL, Zepf M, Kar S, Evans R and Bellei C (2008) Radiation pressure acceleration of thin foils with circularly polarized laser pulses. *New Journal of Physics* **10**, 013021.

Roth M, Cowan TE, Key MH, Hatchett SP, Brown C, Fountain W, Johnson J, Pennington DM, Snavely RA, Wilks SC, Yasuike K, Ruhl H, Pegoraro F, Bulanov SV, Campbell EM, Perry MD and Powell H (2001) Fast ignition by intense laser-accelerated proton beams. *Physical Review Letters* **86**, 436–439.

Shen XF, Qiao B, Zhang H, Kar S, Zhou CT, Chang HX, Borghesi M and He XT (2017) Achieving stable radiation pressure acceleration of heavy ions via successive electron replenishment from ionization of a high-z material coating. *Physical Review Letters* **118**, 204802.

Stark DJ, Toncian T and Arefiev AV (2016) Enhanced multi-MeV photon emission by a laser-driven electron beam in a self-generated magnetic field. *Physical Review Letters* **116**, 185003.

Wagner F, Deppert O, Brabetz C, Fiala P, Kleinschmidt A, Poth P, Schanz VA, Tebartz A, Zielbauer B, Roth M, Stohlker T and Bagnoud V (2016) Maximum proton energy above 85 MeV from the relativistic interaction of laser pulses with micrometer thick CH_2 targets. *Physical Review Letters* **116**, 205002.

Wang HY, Yan XQ, Chen JE, He XT, Ma WJ, Bin JH, Schreiber J, Tajima T and Habs D (2013) Efficient and stable proton acceleration by irradiating a two-layer target with a linearly polarized laser pulse. *Physics of Plasmas* **20**, 013101.

Weng SM, Murakami M and Sheng ZM (2015) Reducing ion energy spread in hole-boring radiation pressure acceleration by using two-ion-species targets. *Laser and Particle Beams* **33**, 103–107.

Wilks SC, Langdon AB, Cowan TE, Roth M, Singh M, Hatchett S, Key MH, Pennington D, Mackinnon A and Snavely RA (2001) Energetic proton generation in ultra-intense laser–solid interactions. *Physics of Plasmas* **8**, 542.

Yan XQ, Wu HC, Sheng ZM, Chen JE and Meyer-ter-Vehn J (2009) Self-organizing GeV, nanocoulomb, collimated proton beam from laser foil interaction at 7×10^{21} W/cm^2. *Physical Review Letters* **103**, 135001.

Yogo A, Mima K, Iwata N, Tosaki S, Morace A, Arikawa Y, Fujioka S, Johzaki T, Sentoku Y, Nishimura H, Sagisaka A, Matsuo K, Kamitsukasa N, Kojima S, Nagatomo H, Nakai M, Shiraga H, Murakami M, Tokita S, Kawanaka J, Miyanaga N, Yamanoi K, Norimatsu T, Sakagami H, Bulanov SV, Kondo K and Azechi H (2017) Boosting laser-ion acceleration with multi-picosecond pulses. *Physics of Plasmas* **7**, 42451.

Yoon PH and Davidson RC (1987) Exact analytical model of the classical Weibel instability in a relativistic anisotropic plasma. *Physical Review A* **35**, 2718–2721.

Zou DB, Zhuo HB, Yu TP, Wu HC, Yang XH, Shao FQ, Ma YY, Yin Y and Ge ZY (2015) Enhanced laser-radiation-pressure-driven proton acceleration by moving focusing electric-fields in a foil-in-cone target. *Physics of Plasmas* **22**, 023109.

https://doi.org/10.1017/S026303461900034X Published online by Cambridge University Press